Parametric study of a metaporous made of solid inclusions embedded in a rigid frame porous material

C. Lagarrigue, O. Dazel, J.-P. Groby and V. Tournat

Laboratoire d'acoustique de l'université du Maine, Bât. IAM - UFR Sciences Avenue Olivier Messiaen 72085 Le Mans Cedex 9
clement.lagarrigue.etu@univ-lemans.fr

With the growing interest for sound absorbing materials, research is brought to optimize porous material whose acoustic absorption coefficient should remain large across a broad frequency range. Embedding rigid inclusions in a porous plate can enhance its acoustical properties and create an efficient sound insulating material for low frequencies. The excitation of additional acoustic modes when periodic arrangements of inclusions are used can lead to enhanced acoustic energy dissipation due to the viscous and thermal effects in the material pores when the wavelength is comparable with the radius of the inclusions. By acting on the characteristics of individual cells (periodicity, shape, type ...), it is possible to combine absorption related to the medium with additional resonant effects at low frequencies. A parametric study is performed in order to determine the influence of the geometry, orientation and resonance frequency of infinitely rigid inclusions embedded in a porous plate. The behavior of these structured materials is computed by finite element method to determine the "optimal" inclusion in order to obtain an efficient absorbing material.

1 Introduction

This work is dedicated to the design of a compact absorbing material with good efficiency over a large frequency band, particularly at low frequencies. Effectively, porous materials (foams) suffer from a lack of absorption at low frequency, when compared to their characteristics at higher frequency, and for normal incidence. The usual way to solve this problem is by multi-layering [3]. The purpose of the present article is to investigate an alternative to multi-layering by embedding a periodic set of resonant rigid inclusions, whose size is not small compared with the incident wavelength for some frequency band, in an otherwise macroscopically-homogeneous porous plate whose thickness and weight are relatively small (i.e., the principal constraints in the design of acoustic absorbing materials). The inclusions and porous skeleton are assumed motionless. This configuration results in a diffraction grating composed of resonant scatterers, and a structure somehow close to the one of a sonic crystal.

The influence of the periodic embeddment of circular cross-section volume heterogeneities in a porous layer backed by rigid backing was previously investigated [5] by use of the multipole method together with a mode matching technique. It was found that this embeddment leads to an increase of the absorption coefficient of the structure due to the excitation of a trapped mode that traps the energy between the periodic set of inclusion and the rigid backing and of the modified mode of the porous plate. Of particular interest is the excitation of this trapped mode which leads to a quasi-total absorption peak for frequency below the so-called quarter-wavelength resonance of the backed porous plate almost independent from the angle of incidence. This trapped mode depends on the characteristics of the porous material, on the dimensions of the unit-cell, the position of the inclusion inside the porous layer and naturally on the inclusion radius. It was shown that for any dimensions of the unit cell, it is possible to find an inclusion radius that enables this trapped mode to be excited. Nevertheless, this embeddment also induces an interaction of the inclusion with its image with respect to the rigid backing that leads to Bragg interference and also to a decrease of the absorption coefficient at this frequency. This frequency only depends on the distance between the center of the inclusion and the rigid backing for circular cross-section inclusions.

Here, we also investigate the influence on the absorption coefficient of the embeddment of different geometries of resonant inclusions in a rigid frame porous layer glued against a rigid wall by means of a FEM code [1]. Such attempt were already discussed in [2], in which a mode matching technique particularly adapted to Cartesian geometry inclusions were developed. The present article aims to provide answers to the following question: Is it possible to find geometry of the resonant inclusion that enable the scatterer to resonate for a frequency that corresponds to an incident wavelength larger than their characteristic dimensions? If so, such a configuration leads to the design of a metaporous material.

2 Formulation of the problem

2.1 Description of the configuration

Both the incident plane acoustic wave and the plate are assumed to be invariant with respect to the Cartesian coordinate x_3. A sagittal x_1-x_2 plane view of the two-dimensional scattering problem is given in Fig.1. Before the introduction of the inclusions, the plate is made of a porous material (e.g., a foam) which is modeled (by homogenization) as a macroscopically homogeneous equivalent fluid $M^{[1]}$. The medium $M^{[0]}$ is considered as a fluid with the characteristics of the air. The inclusions boundaries are considered infinitely rigid (Neumann type boundary condition on the interface porous medium/inclusion) and the medium that fills the inclusions is the same porous material as the surrounding one. As an example of resonant inclusion, a single split ring is considered in Fig.1. The position of the slit of the inclusion is identified by $\alpha^{\{n\}}$, measured counter clock wise from -x_2 axis. Its characteristic dimensions are the opening e and the thickness of the resonator wall, i.e., in the split ring case $r_e^{\{n\}} - r_i^{\{n\}}$. Thus, the plate is macroscopically inhomogeneous, the heterogeneity being periodic in the x_1 direction with period d. In all simulations the rigid backing is placed at the top of the inclusion, at $x_2 = h$. The angle of incidence of the incident plane wave θ^i is measured counter clock wise from the x_2 axis. The initial configuration consists in a rectangular unit cell of 2 cm width. The porous layer is 2 cm hight. The characteristics of the porous materials (Fireflex, Recticel, Belgium) have been determined by traditional methods and are given Table 1.

Table 1: Parameters of the considered porous foam

ϕ	α_∞	$\Lambda(\mu\text{m})$	$\Lambda'(\mu\text{m})$	$\sigma(\text{N s m}^{-4})$	$\nu_c(\text{Hz})$
0.95	1.42	180	360	8900	781

2.2 Method of resolution

Because of the possible complicated geometry of the inclusion, the response and absorption coefficient of each con-

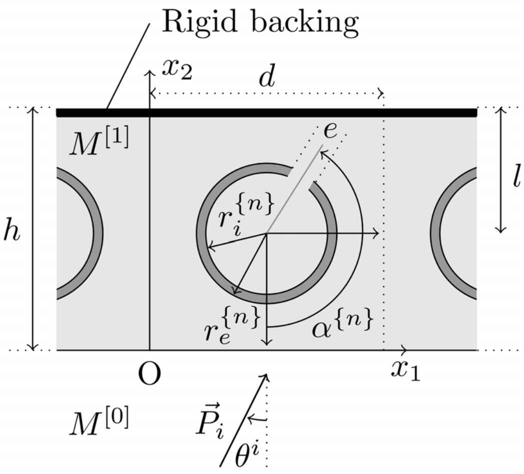

Figure 1: Types of geometry

figuration are simulated with a finite element method (FEM) described in [1] and validated in [1, 5]. Quadratic finite elements are used to approximate the pressure inside the unit cell, thereby leading to a discretized problem of $\mathcal{N}_e$ elements and $\mathcal{N}_n$ nodes. The periodicity relation, i.e., the Floquet condition, is applied on both sides of the discretized domain, i.e., at each nodes of x_1 coordinate 0 and d. For this periodicity relation to be correctly implemented, these two sides are discretized with similar nodes, i.e., identical x_2 coordinates.

3 Parametric study

The influence of the inclusion geometry embedded in a porous media has only been poorly studied till now, most of the previous works were focused on circular cross-section and square-cross section rigid inclusions. Five different geometries are investigated as depicted table3: the split rig, the double split ring, the split rectangle, the split triangle and the split ellipse.

In a first step, we focus on the split ring (SR) of characteristics C1 collected in Table 2 (see inclusions 1 of the Fig. 5). This inclusions have been largely studied in sonic crystals [4, 6, 7] leading to transmission anomalies associated with their resonances.

Table 2: Dimensions for the configuration C1. All values are in centimeter (cm)

	r_i	r_e	d	e	h	l
C1	0.725	0.75	2	0.15	2	1

Two types of phenomena are expected at low frequencies for these resonant inclusions. The first is an increase of the absorption coefficient due to the periodicity of the inclusions. Indeed, the acoustic field will be trapped between the inclusions and the rigid backing for a specific frequency depending of the lattice periodicity and of the position of inclusion. The second is an increase of the absorption due to the resonance of the SR. The peculiar shape of these inclusions could allow resonance for wavelength smaller than the dimensions of the scatterers. At its resonance, the energy will be trapped inside the scatterer resonator.

3.1 Influence of the inclusion orientation

In order to investigate the influence of the neck orientation of this scatterer, simulations are computed on different configurations that only differ from the position of the neck, identified by the angle $\alpha^{\{n\}} = [0, \frac{\pi}{6}, \frac{\pi}{3}, \frac{\pi}{2}, \frac{2\pi}{3}, \frac{5\pi}{6}, \pi]$. The results are summarized in figure 2 where the frequencies of the resonance of the SR and of the trapped mode are plotted as a function of $\alpha^{\{n\}}$. These frequencies are determined by looking at the acoustic field calculated by the FEM at each frequency, and respectively correspond to a maximum of pressure/energy localized in the resonator, and a maximum of pressure/energy localized between the inclusions and the rigid backing. The consequence of the excitation of these two modes are total absorption peaks. When the resonance frequencies of these two modes are close, a coupled mode is excited and only one absorption peak is observed, while two distinct absorption peaks show up when these resonance frequencies are sufficiently spaced in frequency as shown in Figure 3.

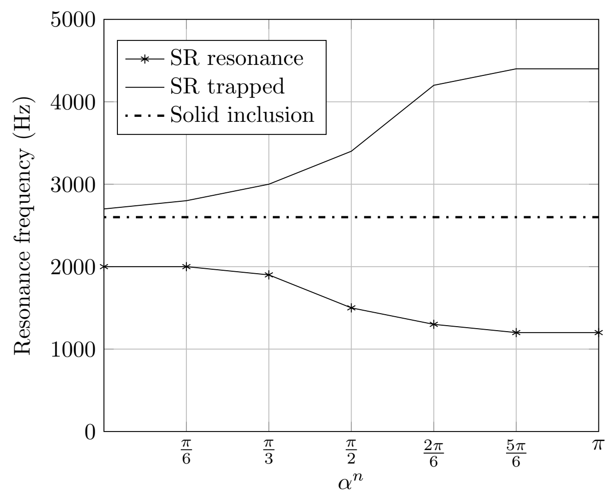

Figure 2: Influence of the orientation angle $\alpha^{\{n\}}$ on the resonance frequencies of the SR and on the frequency of the trapped mode with the configuration C1 (see Tab 2), $\theta^i = 0$, $\mathcal{N}_e = 1602$ and $\mathcal{N}_n = 924$

The angular position of the neck $\alpha^{\{n\}}$ highly influences the resonance frequencies and consequently the frequencies of the absorption maxima in the case of a SR (particularly for values higher than $\pi/2$).

First, the resonance frequency of the SR decreases when $\alpha^{\{n\}}$ increases. The minimum frequency is reached for $\alpha^{\{n\}} = \pi$. This can be explained by analogy with an Helmholtz resonator where the volume of the cavity acts as a spring, and the volume of the neck acts as a mass. When the length of the neck increases, the mass increases and consequently the resonance frequency decreases. Here, the surrounding inclusions together with the rigid backing act as an extension of the neck when the neck is in the upper half space, i.e., when $\alpha^{\{n\}}$ is larger than $\pi/2$. In particular, when $\alpha^{\{n\}} = \pi$, the incident wavelength in the air medium is 23 cm at the resonant frequency of the scatterer, i.e. 1500 Hz. The structure being 2 cm thick, this means that this arrangement enables a quasi-total absorption of an incident wavelength more than 10 times larger than the medium thickness, therefore creating a metaporous material. In fact, this very large wavelength when compared to the structure thickness, is due to the structure itself enabling a resonance of SR at low frequency thanks to the periodicity (i.e. the surrounding SR and the rigid backing, but also to the properties of the material itself in which the wavelength is larger than the incident one because the particle velocity is smaller in the rigid frame porous material than in the air medium).

Secondly, the resonance of the trapped mode increases with $\alpha^{\{n\}}$. When $\alpha^{\{n\}}$ is less than to $\pi/2$ the acoustic field trapped between the rigid backing and the inclusion is almost unchanged compared to the case of a rigid inclusion. The acoustic field is closed to be uniformly distributed along the axis x_2 (see Fig. 3a). When $\alpha^{\{n\}}$ is more than to $\pi/2$ the neck of the resonator introduces another distribution of the pressure field and acts as an anomaly. For $\alpha^{\{n\}} = \pi$, this anomaly is maximum. The acoustic field is still trapped between the rigid backing and the inclusions but the pressure is forced to be distributed in a slightly different way.

The frequency of the trapped mode seems to increase faster than the frequency of the SR resonance.

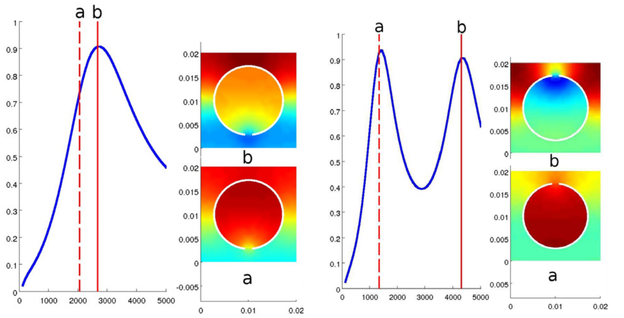

(a) $\alpha^{\{n\}} = 0$ (b) $\alpha^{\{n\}} = \pi$

Figure 3: Pressure field as a function of the position of the hole with a normal incident wave and with dimensions of the configuration C1 (see Tab. 2), $N_e = 1602$ and $N_n = 924$

A particular feature of the trapped mode and of the resonance mode of the SC are independent form the angle of incidence. Figure 4 presents the absorption coefficient of the structure C1 for various angles of incidence. The frequency and amplitude of absorption peaks associated to the excitation of these modes are almost independent of the angle of incidence. The SR is an inclusion type that presents tunable

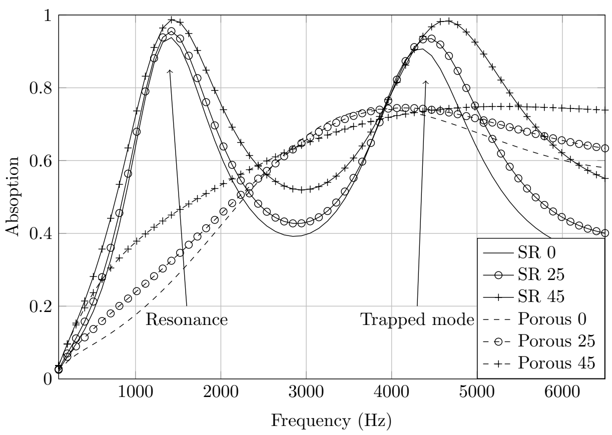

Figure 4: C1 - Influence of the angle of incidence of the incident wave on a split ring cell with $\alpha^{\{n\}} = \pi$ and with dimensions of the configuration, $N_e = 1602$ and $N_n = 924$

properties as a function of the position of the neck. This angular dependence could be used to enlarged the frequency band over which the absorption is maximum by controlling the resonance frequencies of the scatterers in a more complex arrangement when coupled with the trapped mode.

3.2 Influence of the geometry of the inclusion

It has been shown in [2] that the frequency and specific features of the trapped mode are almost identical between square and cylindrical cross-section inclusions. Nevertheless, the geometry of the inclusions could have an influence on the repartition of the scattered waves at higher frequencies, particularly around the Bragg interference frequency. Moreover, in the following, some of the considered inclusions could resonate. Five geometries are tested (see Fig.5), each time for a non-resonant (not exposed in this paper) and a resonant version for all values $\alpha^{\{n\}}$. All types of inclusions are designed in order to have the same volume, the same thickness, the same e and consequently almost the same resonance frequency. The geometric barycenter is kept around the central point of unit cell $(d/2, h/2)$.

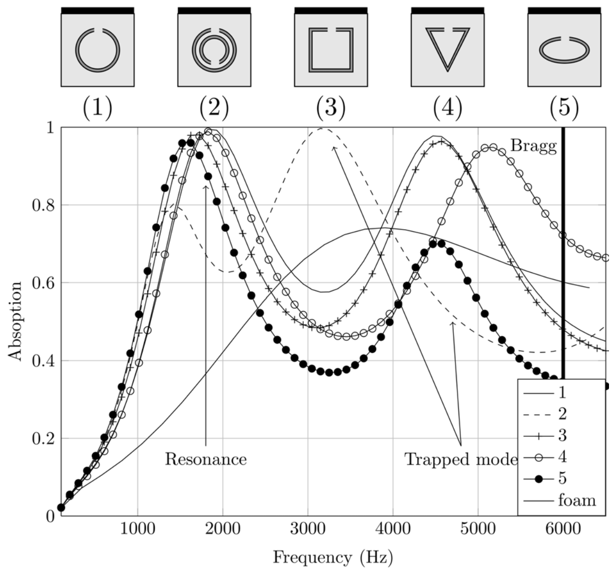

Figure 5: Comparison of different types of inclusion geometries for $\alpha^{\{n\}} = \pi$ and for a normal incident wave. Dimensions of the inclusions are provided in Tab.3 (configurations C2 to C6), $N_e = 2170$ and $N_n = 1208$

A first remark concerns the double split ring resonator (DSR). When compared with the SR, an additional phenomenon can be noticed and is related to an increase of the absorption coefficient due to a resonance of the neck (see Fig.6d). At this frequency the neck resonates and can be considered as a quarter wavelength resonant wave guide. A second remark concerning this resonator is that the resonance frequency of a DSR is almost independent of $\alpha^{\{n\}}$. The reason is that the additional neck length introduced by the surrounding inclusions and rigid backing is negligible when compared with the initial neck length of this resonator. On the opposite, $\alpha^{\{n\}} = 0$ influences the resonance frequency of the inclusions for all the other geometries in a similar way as the SR type inclusions.

The figure 5 shows the absorption coefficient of all the resonant geometries considered here for an angle $\alpha^{\{n\}} = \pi$. The differences are quite small around the resonance of the inclusion and trapped mode excitation frequency and all geometry (except the n°2) exhibit the same behavior. The geometries that remain the most interesting are the n°1 and n°4 that offer the higher absorption coefficient or the best tunable potential.

3.3 Creation of a supercell

The tunability of a SR inclusion as a function of $\alpha^{\{n\}}$ is now used to design a supercell composed of SR and DSR inclusions with different neck positions $\alpha^{\{n\}}$. The idea is to enlarge the frequency band of enhanced absorption coefficient by considering a combination of resonant scatterers of different, but also closed resonance frequencies, whose resonance would combined one with each other but also with the trapped mode. This supercell could be efficient for the absorption of wide frequency band noises.

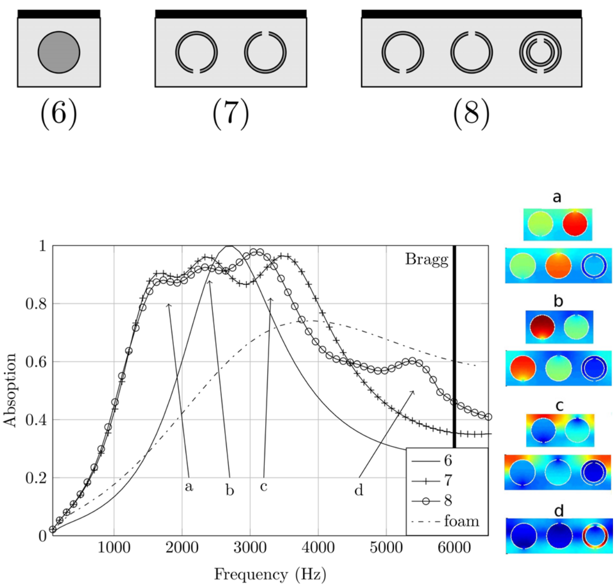

Figure 6: Comparison of different types of supercells for a normal incident wave. Dimensions of the configuration are C1 and C1' (see Tab.2 and Tab.3), cell n°7: $\mathcal{N}_e = 3118$, $\mathcal{N}_n = 1743$ and cell n°8: $\mathcal{N}_e = 3992$, $\mathcal{N}_n = 2305$

The basic cell is the one previously studied. The distance between two inclusions is kept at $d = 2$ cm. The external radius is $r_e = 1.5$ cm. The supercell is composed of an arrangement of this basic cell with various geometries and positions of the neck. The periodicity of the supercell is also enlarged but the "apparent" periodicity is closed to 2 cm. The frequency of and pressure field at the trapped mode excitation is also slightly changed when compared to the previously studied configurations

The cell n°6 is considered as the reference one. It is composed of a periodic set of rigid inclusions and only the trapped mode can be noticed for this configuration.

For the frequency band of enhanced absorption to be the largest as possible, the resonance frequencies of the scatterers should not be too close one from each other in order not to have a single absorption peak. They should not be too far one from each other in order not to have an array of peaks. A simulation are performed with a supercell composed of four inclusions, oriented with $\alpha^{\{n\}} = [\frac{\pi}{2}, \frac{2\pi}{3}, \frac{5\pi}{6}, \pi]$ for $n = [1, 2, 3, 4]$ but the resonance frequencies were too closed one from each other. This results in a narrow frequency band of absorption around 1500 Hz and another maximum of absorption around 4000 Hz associated with the excitation of the trapped mode. In the supercell n°8 the resonance frequency due to the quarter-wave resonator is too far and not enough efficient to excite a coupled mode with the trapped and the resonance mode. The configuration n°7 is the more efficient and attenuates noises in a frequency band between 1500 Hz and 3500 Hz with an absorption coefficient of 0.9. The resonances of each resonator and of the trapped mode are close enough to excite some coupled modes to which provides a large absorption coefficient on a wide frequency band.

Conclusion

The influence of the embeddement of resonant periodic inclusions of various geometries in a porous sheet attached to a rigid plate on the acoustic absorption has been studied numerically. In addition to the absorption features related to the excitation of a trapped mode which lead to a quasi-total (close to unity) absorption peak below the quarter-wavelength resonance frequency, it is shown that an additional, even lower frequency peak of absorption, associated with the resonance of the scatterer, can be obtained.

This particular feature enables the design of small dimension absorption packages. In particular, it is shown on different geometries of split resonators that the resonance frequency depends on the angular position of the neck α^n in the arrangement. For values of α^n higher than $\frac{\pi}{2}$ the surrounding inclusions and the presence of the rigid backing virtually increase the length of the resonator neck leading to a decrease of the resonance frequency around 1500 Hz for a 2 by 2 cm unit cell.

This phenomenon offers possibility of frequency tuning very interesting for acoustic absorbing of large frequency band noises. In the case of more than one inclusion per spatial period, it is found that the quasi-total absorption peak on a wide frequency band can be reached by using split rings with two different orientations. In this case the characteristic dimensions are correctly chosen to excite the different phenomena in frequency bands close enough to observe coupled modes that maintain this high absorption coefficient from 1500 Hz to 3500 Hz. The wavelength at this frequency band is between five and ten times larger than the characteristic dimensions of the unit cell which makes this layer "metaporous".

The method offers an alternative to multi-layering and double porosity materials for the design of sound absorption packages and would be of large interests for lower frequency applications. The next step is to validate experimentally the results observed in this paper.

References

[1] J.F. Allard, O. Dazel, G. Gautier, J.P. Groby, and W. Lauriks. Prediction of sound reflection by corrugated porous surfaces. *The Journal of the Acoustical Society of America*, 129:1696, 2011.

[2] J.-P. Groby et Y. AurĂŠgan B. Nennig, Y. Renou. A mode matching approach for modeling 2d porous grating with rigid or soft incluions. *Journal of the Acoustical Society of America*, 2012. Accepted for publication.

[3] L.M. Brekhovskikh and R.T. Beyer. Waves in layered media. 4, 1960.

[4] D. P. Elford, L. Chalmers, F. V. Kusmartsev, and G. M. Swallowe. Matryoshka Locally Resonant Sonic Crystal. *ArXiv e-prints*, page 1102.0399v1, February 2011.

[5] JP Groby, O. Dazel, A. Duclos, L. Boeckx, and L. Kelders. Enhancing the absorption coefficient of a backed rigid frame porous layer by embedding circular periodic inclusions. *Journal of the Acoustical Society of America*, 130(6):3771, 2011.

[6] AB Movchan and S. Guenneau. Split-ring resonators and localized modes. *Physical Review B*, 70(12):125116, 2004.

[7] V. Romero-García, JV Sánchez-Pérez, and LM Garcia-Raffi. Tunable wideband bandstop acoustic filter based on two-dimensional multiphysical phenomena periodic systems. *Journal of Applied Physics*, 110:014904, 2011.

A Dimensions for the different configurations

Table 3: Dimensions for the different configurations used in this article. All values are in centimeter (cm).

C1'	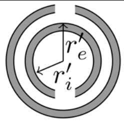	r_i	r_e	r'_i	r'_e	e
		0.725	0.75	0.53	0.57	0.15
C2	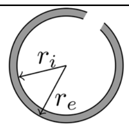	r_i	r_e	e		
		0.57	0.61	0.1		
C3	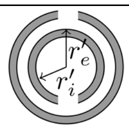	r_i	r_e	r'_i	r'_e	e
		0.57	0.61	0.43	0.47	0.1
C4	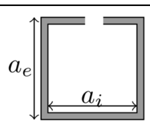	a_i	a_e	e		
		1.01	1.1	0.15		
C5	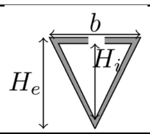	b	H_i	H_e	e	
		1.65	1.32	1.43	0.15	
C6	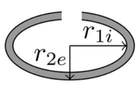	r_{1i}	r_{1e}	r_{2i}	r_{2e}	e
		0.74	0.82	0.44	0.49	0.1